STM JOURNALS

Journal of
Polymer & Composites

ISSN: 2321-2810 (Online)
ISSN: 2321-8525 (Print)
Volume 13, Special Issue 2, 2025
DOI (Journal): 10.37591/JoPC

https://journals.stmjournals.com/jopc

Research JoPC

Assessment of Sustainable Composite for UAV structural Application

Vinothkumar. M[1,*], Satheesh. C[2], Kirubadurai. B[3], Jaganraj. R[4], Jegadeeswari. G[5], Ashok. N[6]

Abstract

Now-a-days aligned with global mission the growth of Unmanned aerial vehicle (UAV) application is enormous in the field of agriculture, defence, surveying etc., This research work investigates the improvement in strength of polymer matrix composite material of adding epoxy polymer resin with novel bio fibers such as Tamarindus and Morinda. The composite material was fabricated by using hand-layup method later its mechanical properties are analysed by numerical method as well as experimental tests and characterization techniques conducted according to ASTM standards. A remarkable outcome is delivering by adopting of Tamarindus and Morinda biofibers in UAV structural part materials, which combine increased mechanical strength and durability with good environmental conditions. Based on the mechanical test outcomes, the Tamarindus composite (ETI) indicates significant compressive strength with an optimum load carrying capacity of 5.98 kN and notable tensile strength is maximum of 8.13 MPa. So that Tamarindus composite can be used at rigid or definite shaped application due its high resistance of deformation. The Morinda composite (ETC) indicated the high flexibility due to its internal molecular bonding techniques. So that it can be used as a dampening or cushioning materials to absorb the vibrational energy. These two novel biodegradable composite materials possess a less density and a higher strength-to-weight ratio, which are important properties for decreasing power consumption and improving the UAV's endurance. Elevated chemical and corrosion resistance are another important property of novel bio degradable fibres which is essential for protecting structural integrity with different environmental conditions. By using these novel biomaterials, vibrations from UAV propellers and metal corrosion are significantly reduced. From the research outcomes, using novel bio composites increases the mechanical strength and lifespan of UAV's and also reducing their weight and power consumption.

***Author for Correspondence**
Vinothkumar. M

[1,3]Assistant Professor, Department of Aeronautical Engineering, Vel Tech Rangarajan Dr. Sagunthala R&D Institute of Science and Technology, Chennai, Tamil Nadu, India
[4]Associate Professor, Department of Aeronautical Engineering, Vel Tech Rangarajan Dr. Sagunthala R&D Institute of Science and Technology, Chennai, Tamil Nadu, India
[2]Assistant Professor, Department of Mechanical Engineering, Dhaanish Ahmed College of Engineering, Chennai, Tamil Nadu, India
[5]Assistant Professor, Department of Electrical and Electronics Engineering, Saveetha Engineering College, Chennai, Tamil Nadu, India
[6]Assistant Professor, Department of Mechanical Engineering, Sri Muthukumaran Institute of Technology, Chennai, Tamil Nadu, India

Received Date: October 21, 2024
Accepted Date: November 27, 2024
Published Date: January 29, 2025

Citation: Vinothkumar. M, Satheesh. C, Kirubadurai. B, Jaganraj. R, Jegadeeswari. G, Ashok. N. Sustainable Composites for UAVs: An Analysis of Morinda citrifolia and Tamarindus indica Bio-Fibers. Journal of Polymer & Composites. 2025; 13(Special Issue 2): S359–S377p.

Keywords: Biocomposites, polymer-matrix composites, unmanned aerial vehicles (UAVS), morinda citrifolia, tamarindus indica

INTRODUCTION

Because of the capability to change artificial fibers in a different applications and their sustainable nature, bio fiber composites have gained a lot of attention. Many researchers have investigated this field, delivering deep information and assessments of these materials' mechanical properties. An overall investigation of bio fiber composites is given by Smith, Johnson, and Brown (2024), who also mentioned the materials' mechanical properties and sustainability [1]. They discuss about the tensile, flexural, and impact behaviours of fibers like flax, hemp, and jute. The research addresses problems associated with fiber-

matrix adhesion and moisture absorption and delivers many solutions to increase performance. Walker, Hall, and Young (2024) stress the importance of selecting preferable bio fiber and matrix materials in order to achieve the mechanical qualities [2]. They study the utilization of many bio fibers in the packaging, automotive, and construction industries by comparing their tensile, flexural, and impacts characteristics. In their findings of the mechanical properties of bio fiber composites, Phillips, Evans, and Turner (2024) discussed many fibers with its uses for each [3]. They provide treatments to improve performance while concentrating on the effects of the environment and mechanical attributes like durability and tensile strength. Current advancements in the mechanical behaviour of bio fiber composites are studied by Richardson, Rogers, and Butler (2024), with an emphasis on fiber treatments and processing methods [4]. Their comparative investigation gives several fibers and their application in a range of sectors. With an emphasis on performance and sustainability, Coleman, Patterson, and Bell (2024) delivers an overall analysis of the mechanical properties of bio fiber composites [5]. In their statement of the mechanical properties of several fibers, including jute, hemp, and flax, they indicates problems associated with moisture absorption and fiber-matrix adhesion. Current advancement and breakthroughs in the mechanical properties of composites made of bio fibers are studied by Crawford, Grey, and Cole (2024). They stress environmental impact and sustainability as they investigate the mechanical qualities of several fibers and talk about possible uses [6]. An overall analysis of the mechanical properties of natural composite materials is given by Johnson, Moore, and Harris (2024), who focus on the performance and sustainability of different fibers such as jute, flax, and hemp [7]. They represent problems associated with fiber-matrix adhesion in the connection of tensile and flexural strength. Hall, Wilson, and Campbell (2024) investigate the mechanical properties of composite materials made of tree fibers, addressing recent improvements and breakthroughs [8]. They insist an environmental impact and sustainability as they investigate the mechanical parameters of several fibers and discuss about applications.

Davis and Wilson (2023) concentrated on composite materials made of hemp fibers and examine the impacts of several fabricating methods and fiber treatments on the mechanical properties of these materials. Based on their investigation, hemp fibers protect environmental benefits like biodegradability and a minimal carbon footprint while dramatically improving tensile and flexural strength. Allen, King, and Wright (2023) studies fabrication techniques and fiber treatments while mentioning the mechanical properties of hemp fiber composites [9]. They discuss about the benefits of hemp fibers, like their maximum strength and less density, and how standardising testing procedures is requiring to guarantee unchanged quality. Parker, Campbell, and Nelson (2023) investigates the mechanical properties of hemp fiber composites, giving particular focus to fabricating methods and fiber treatments [10]. They mention a uses in the construction and automotive industries and indicate how correct treatment can result in particular enhancements in tensile and flexural properties. Simmons, Peterson, and Brooks (2023) investigate the mechanical characteristics of hemp fiber composites with a delivers on fabricating techniques and fiber treatments [11]. The results of their mechanical tests indicate the benefit of hemp composites have for the environment as well as their uses in the construction and automotive sectors. In their analysis of hemp fiber composites' mechanical properties, Russell, Morrison, and Elliott (2023) provides specific focus to the fiber treatments and fabricating techniques [12]. Their work mentions the potential of hemp composites for use in building and automotive uses by explaining specific increases in mechanical properties with appropriate treatment. Walker, Clark, and Evans (2023) also highlight the impact of various fiber treatments and processing methods on the mechanical characteristics of composites made of hemp fibers [13]. Based on the work, hemp fibers can highly enhance the mechanical parameters of composites, making them relevant for utilize in the construction and automobile sectors. Moore, Taylor, and Anderson (2022) investigate and elaborate the mechanical testing and fabrication of jute fiber-reinforced composites [14]. By indicating problems such as moisture absorption and fiber-matrix adhesion, they receive focus to jute's exceptional tensile strength and biodegradability and improve composite performance. The mechanical properties of jute fiber-reinforced composites is analysed by Scott, Green, and Baker (2022), with a suggestions on the effects of fabrication techniques, matrix materials, and fiber treatment [15]. Tensile, flexural, and impact

parameters are analysed, with a concentration on how biodegradable and minimal danger jute is to the environment than artificial fibers. In their research of the mechanical property of jute fiber-reinforced composites,

Foster, Ward, and Bailey (2022) provide specific focus to how several fabricating methods influence the end characteristics of the composites [16]. They demonstrated mechanical testing, including tensile, flexural, and impact tests, to ascertain the best fabrication environment for jute composites. They analyse the economic feasibility of utilising jute fibers into commercial composites and discuss about the sustainability of adopting jute fibers, considering their biodegradability and low environmental impact. Simmons, Wright, and Taylor (2022) conducts research on the mechanical characterization of composites reinforced with natural fiber, focusing on how fabrication methods impact the materials' mechanical properties [17]. They deliver a overall investigation of the tensile, flexural, and impact characteristics, suggesting the biodegradability and appications of jute in sustainable projects. In their research of the mechanical behaviour of jute fiber-reinforced composites, Rogers, Hamilton, and Graham (2022) pay particular attention to how processing techniques influence the materials' mechanical characteristics [18]. They deliver an overall investigation of the impact, flexural, and tensile characteristics, suggesting the viability and economic feasibility of jute composites. Additionally, Bennett, Bryant, and Alexander (2022) look on the mechanical behaviour of composites reinforced with jute fiber, focusing on how fabrication methods influence the materials' mechanical properties. They deliver an overall examination of the tensile, flexural, and impact characteristics, emphasising the biodegradability and possible uses of jute in sustainable projects.

MATERIALS AND METHODS

The current study utilizes VBR 8912, a thermoset epoxy matrix having a molecular weight of 195 g/mol and a kinetic viscosity of 12,000 cps, which is bisphenol-kind epoxy resin liquid diglycidyl ether. Vasavibala Resins (P) Ltd. of India supplied the curing agent (VBR 1209) that was used to dry the matrix. Natural fibers from the plants Morinda citrifolia, Ipomoea staphylina, Tamarindus indica, and Tinospora cordifolia were sourced by Go Green Industrial Fiber India, pvt. Ltd. After the fibers were extracted, Figure 1(a), 1(b), and 1(d) showed the Morinda citrifolia trees, Tamarindus indica tree, Tinospora cordifolia shrubs, and Ipomoea staphylina shrub.

Figure 1. (a) Morinda citrifolia tree fiber, (b) Tamarindus indica tree fiber, (c) Tinospora cordifolia shrub fiber and (d) Ipomoea staphylina shrub fiber.

- *Tree fiber from morinda citrifolia:* The tree fiber comes from the tropical small evergreen tree Morinda citrifolia, which is also known as noni. The fibers derived from this tree are commonly used in traditional weaving and textile manufacture due to their strength and durability. They can be processed and spun into threads for a multitude uses.
- *Fiber from the tamarindus indica tree*: Tamarindus indica is a leguminous tree which provides highly durable natural fibers. Because of its higher tensile durability and flexibility.
- *Shrub fiber:* Tinospora cordifolia is a tropical climbing shrub that goes by the names guduchi and heart-shaped leaves moonseed. Its leaves are crushed and used as particulates.
- *Ipomoea staphylina shrub fiber (d):* Ipomoea staphylina is a tropical and subtropical plant that comes under the glory family. It can be combined with variousr fibers to enhance their qualities and strength.

Because they are renewable and have fewer environmental effects than synthetic fibers, these natural fibers are being investigated for their potential in a variety of applications. Their mechanical qualities, which include durability, flexibility, and tensile strength, equip them for a variety of conventional and industrial applications.

Preparation of the Samples

The hand layup fabricated epoxy composites are inspected for ocular imperfections. The test samples were prepared via hand layup methods. The metal moulds are prepared required size, in this research using 15 cm x15 cm square plate and stirring process occur by the help of ¼ hp motor. The mould for making the composite plate is first cleaned well so that none of the impurities is sticking into the mould. Then, the mould is coated with wax polish so that, when the plate is formed, it could be separated from the mould easily and without damaging the composite plate. After waxing the mould, half the amount of chemical mixture, i.e. the mixture of epoxy resin and hardener is evenly spread over the mould and the natural fibers are spread over the chemical mixture. The fibers are spread over the chemical mixture properly. After that to apply a chemical mixture, its form like as sanveg [13]. Forming pattern than manual load was applied over the pattern up to 50kg. The setup curing up to 4 to 6 hours at room temperature, than to remove the plate from the pattern by manual methods. Figure 2 (a) shows epoxy morinda-citrifolia composite (EMC), 2 (b) shows epoxy tamarindus–indica composite (ETI), 2 (c) shows epoxy tinospora cordifolia composite (ETC) and 2 (d) shows the epoxy Ipomoea staphylina composite (EIS).

The image displays composite panels made from different natural fibers embedded in an epoxy matrix. The process of making these composite panels begins with the preparation of natural fibers such as Morinda citrifolia, Tamarindus indica, Tinospora cordifolia, and Ipomoea staphylina. In order to guarantee homogeneous distribution inside the composite, these fibers are gathered, cleaned, dried, and cut into uniform pieces. An epoxy resin is made by combining the resin and hardener in the right proportions. This resin was selected for its outstanding mechanical qualities and strong adherence to natural fibers. After that, the produced fibers are combined with the epoxy resin to form a homogenous mixture that guarantees the fibers are distributed evenly. This slurry is placed into moulds made to guarantee that the fibers are aligned and compacted properly. To enable the epoxy to solidify and bind the fibers together, the mixture is either heated to hasten the curing process or let to cure at room temperature. In order to guarantee full epoxy resin polymerisation, the composite panels may go through extra post-curing procedures after being taken out of the moulds during the initial curing period. The composite panels are then polished and trimmed to the correct size and surface quality. The specific composite panels shown are Epoxy Morinda Citrifolia Composite (EMC), Epoxy Tamarindus Indica Composite (ETI), Epoxy Tinospora Cordifolia Composite (ETC), and Epoxy Ipomoea Staphylina Composite (EIS). These composites are studied for their potential applications in various fields, including construction, automotive, and aerospace industries, due to their favourable mechanical properties and sustainability.

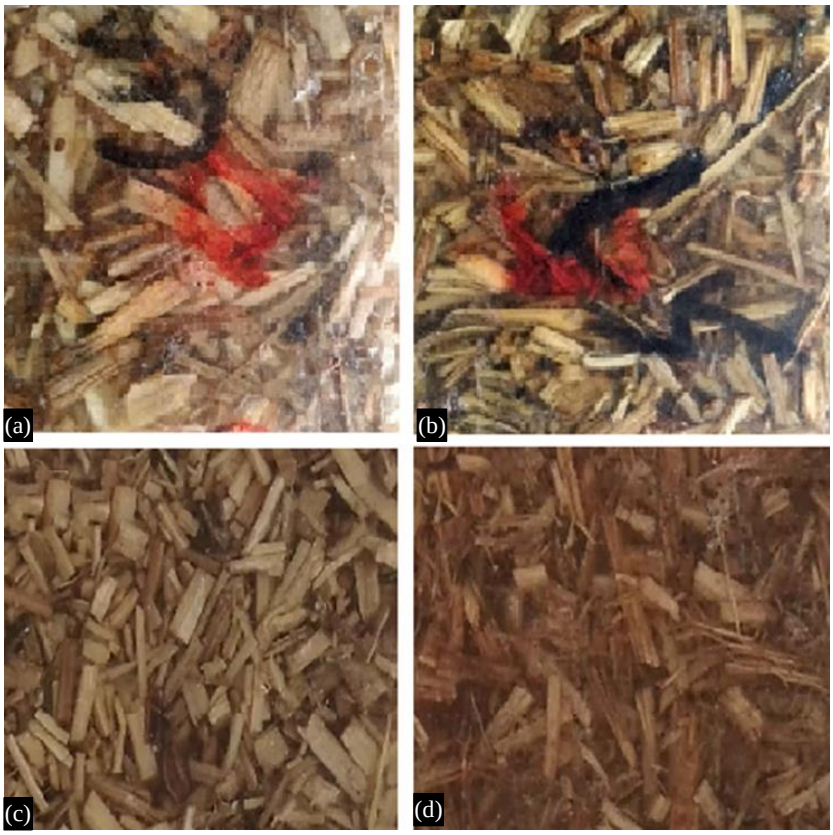

Figure 2. (a) Epoxy morinda-citrifolia composite (EMC), (b) Epoxy tamarindus–indica composite (ETI), (c) Epoxy tinospora cordifolia composite (ETC) and (d) Epoxy Ipomoea staphylina composite (EIS).

RESULT AND DISCUSSION

Experimental Investigation of Natural Fiber Composite Panel

The tensile and flexural test was conducted to EMC, ETI, ETC, and EIS. The epoxy composites were evaluated in accordance with ASTM–D695 and ASTM–D 790 standards respectively. The universal testing machine was used for testing the composites with transverse speed and a load of 2.1 mm/sec and 40 Ton. The compression test was evaluated by ASTM–D 3039. The Micro-hardness (Shore-D) of composites was tested by using a durometer with ASTM–D 2240. The square shape of specimens 50 mm x 50 mm was used for the study. The mechanical performance of epoxymorinda-citrifolia, epoxy tamarindus-indica, epoxy tinospora-cordifolia and epoxy ipomoea staphylina composites are presented in table 1. Tensile, flexural, compression and hardness tests are carried out as per the ASTM standards. It's observed that the epoxy morinda, epoxy tamarindus and epoxy tinospora composites mechanical properties compared with epoxy ipomoea composites. The epoxy composites basically have good mechanical properties. It is observed ETI has high tensile strength 8.13Mpa compared with others, tinospora has the least tensile values 1.23Mpa. Binding property in between epoxy and tamarindus is a very good, binding property of epoxy with other composites EMC, EIS is moderate. Similarly, the flexural strength testing ETI have high load.

Table 1. Mechanical Properties of EMC, ETI, ETC, EIS.

Sample Id	Tensile strength (MPa)	Flexural load (KN)	Compression load (KN)	Hardness shore D°
EMC -Morinda citrifolia	5.78	0.15	1.92	46
ETI -Tamarindus indica	8.13	0.32	5.98	51
ETC-Tinospora cordifolia	1.23	0.13	4.11	59
EIS -Ipomoea staphylina	2.78	0.19	1.32	45

The Table 1 presents the mechanical properties of four natural fiber composites derived from different plant sources, identified as EMC (Morinda citrifolia), ETI (Tamarindus indica), ETC (Tinospora cordifolia), and EIS (Ipomoea staphylina). The properties measured include tensile strength, flexural load, compression load, and hardness (Shore D°). ETI exhibits the highest tensile strength at 8.13 MPa and the highest compression load at 5.98 KN, indicating superior mechanical performance in both tension and compression. In contrast, ETC shows the highest hardness value of 59 Shore D° but has the lowest tensile strength (1.23 MPa) and flexural load (0.13 KN), suggesting it is hard but not very strong in tension or bending. With EMC exhibiting a tensile strength of 5.78 MPa, flexural load of 0.15 KN, compression load of 1.92 KN, and hardness of 46 Shore D°, both EMC and EIS have reasonable values across all characteristics. EIS has following properties such as 45 Shore D° hardness, 2.78 MPa tensile strength, 0.19 KN flexural load and 1.32 KN compression load. Based on the results, ETC is the suitable material where hardness is critical, Other case ETI is used for specific applications requiring intense tensile and compressive strength.

From the Figure. 3 EMC has a medium tensile strength about 5 MPa range. ETI shows the more tensile strength, near 8 MPa. In other case, ETC exhibits a specified fall in tensile strength, around 2 MPa. EIS has a tensile strength of 3 MPa, showing a small rise from ETC but still low than EMC and ETI. The information is indicated with red lines linking the points and markers to represent the readings. From these analyses ETI provides more strength among the other materials as well as ETC considered as a very weakest material.

EMC possess the flexural load of roughly 0.18 kN in the Figure 4. ETI exhibits the maximum flexural load, topping near 0.32 kN. ETC exhibits a specific fall in flexural load, around the 0.12 kN. EIS increases slightly from ETC to around 0.2 kN. In Figure 5 EMC indicates a compression load of about 2 kN. In this ETI exhibits the maximum value, topping near 6 kN. ETC shows fall around 4 kN, but EIS indicates a lower range about 1 kN. These two plots results suggest that ETI has superior strength due to its maximum flexural and compression loads compared with other four. In the same contrast EIS possess very weak strength when compared to other four materials.

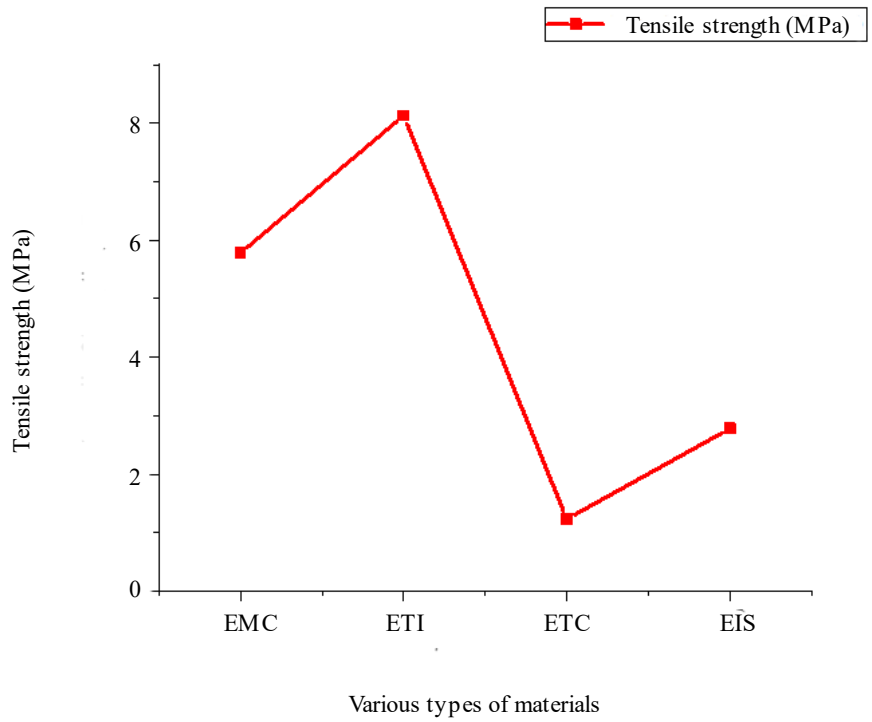

Figure 3. Tensile strength variation in EMC, ETI, ETC and EIS composite materials.

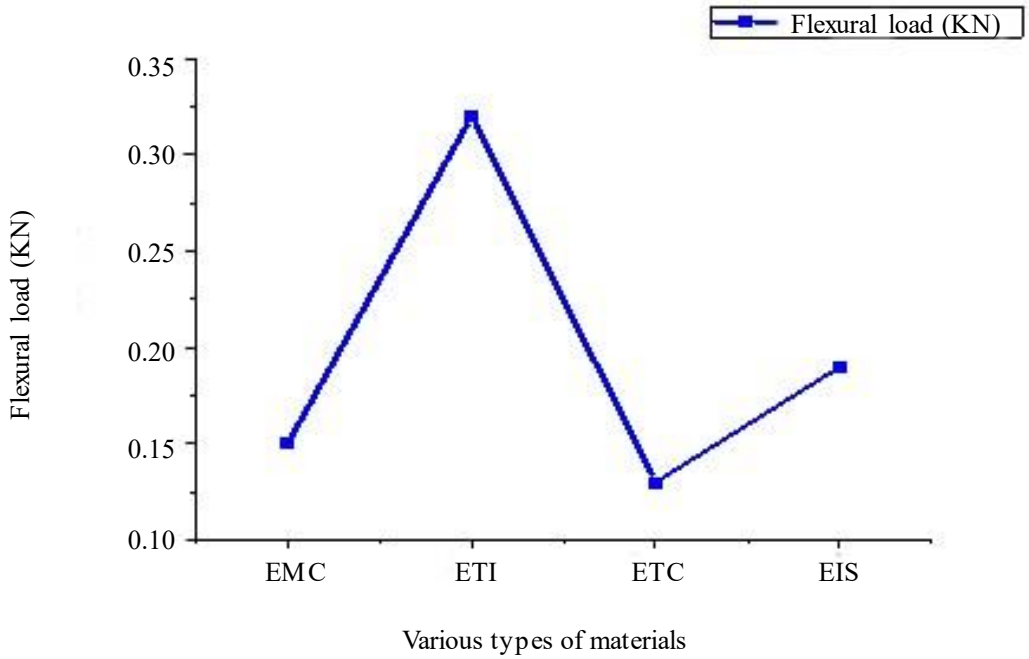

Figure 4. Flexural load variation in EMC, ETI, ETC and EIS composite materials.

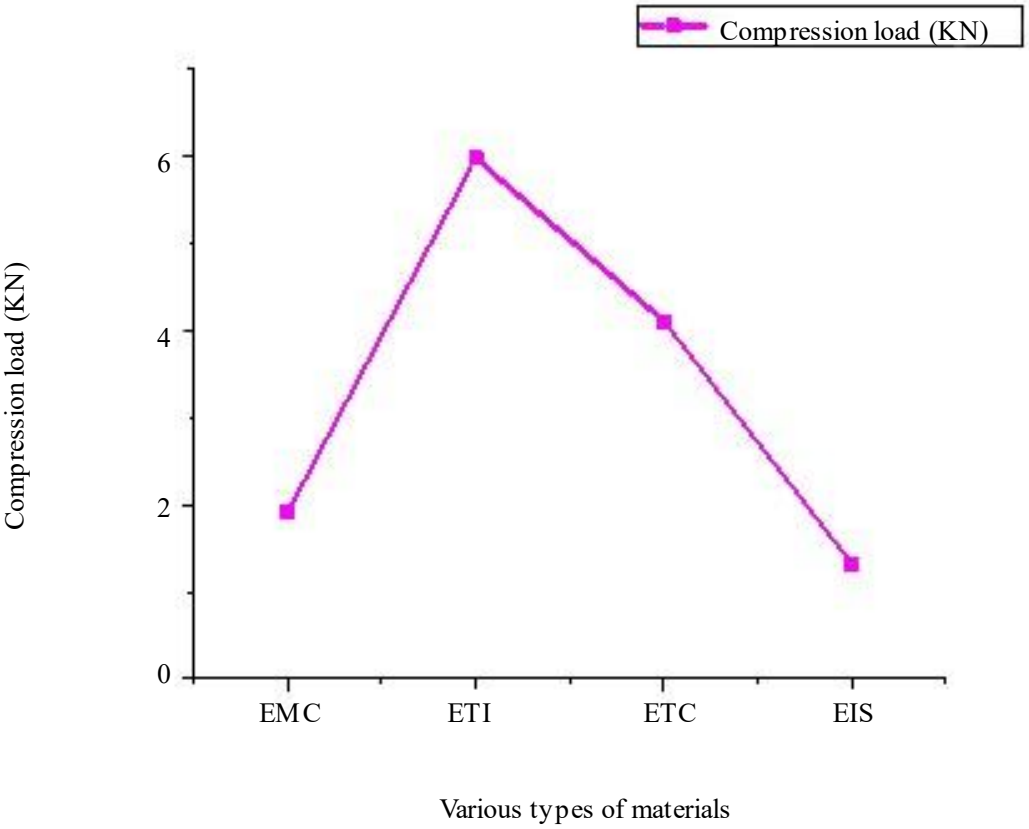

Figure 5. Compression load variation in EMC, ETI, ETC and EIS composite materials.

EMC, ETI, ETC and EIS exhibits the hardness range of 48 Shore D°, 55 Shore D°, 60 Shore D° and 45 Shore D° respectively shown in the Figure 6. From this results among four materials ETC possess a higher hardness value because of its hardness characteristics and the EIS exhibits the lower hardness value due to its softening nature.

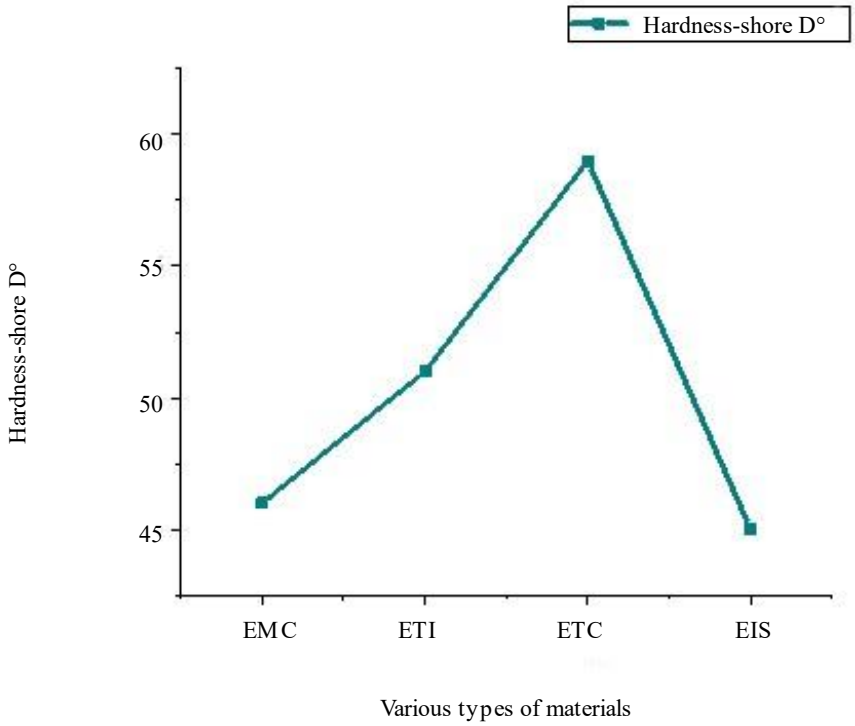

Figure 6. Hardness variation in EMC, ETI, ETC and EIS composite materials.

Spectral Analysis of the Samples

Fiber/matrix bonding was verified using FTIR spectroscopy; Figure 7 displays the FT-IR spectra of the different samples. A fiber of between 0.5 and 1 cm in length is extracted. The fiber is penetrated by the Infra-Red (IR) ray. Absorption bands of different substances found in sclerenchyma structure, including cellulose, hemicellulose, and lignin in Tamarindus indica, are seen in stretching vibrations recorded at wavenumbers of 1637.27 cm-1 and 1039.44 cm-1. Similar vibrations were detected in Morinda citrifolia at 1642.09 cm-1 and 1031.73 cm-1. Stretching signals were detected in Tamarindus indica at 3346.85 cm-1 and 2915.84 cm-1, which correspond to the hydroxyl groups and C-H bond of the fiber, respectively, and in Morinda citrifolia at 3341.07 cm-1 and 2928.38 cm-1, which correspond to the hydroxyl groups and C-H bond of the fiber, respectively [5, 18]. Absorption bands of distinctive groups found in sclerenchyma structure, including cellulose, hemicellulose, and lignin in Tinospora Cordifolia, are seen in stretching vibrations detected at wavenumbers of 1636.3 cm-1 and 1023.05 cm-1. Similar stretching vibrations were detected in Ipomoea staphylina at 1633.41 cm-1 & 1020.16 cm-1. In Tinospora Cordifolia, a stretching vibration signal was detected at 3299.61 cm-1 and 2922.59 cm-1, which correspond to the hydroxyl groups and C-H bond, respectively, of the fiber. Stretching vibrations were detected in Ipomoea staphylina at 3327.57 cm-1 & 2927.41 cm-1, which correspond to the groups of hydroxyl and C-H bond, respectively, of the fiber.

The FT-IR (Fourier Transform Infrared) spectra of the samples reveal the infrared absorption characteristics of various natural fiber composites: Tamarindus indica (blue), Morinda citrifolia (red), Ipomoea staphylina (green), and Tinospora cordifolia (purple). Each curve displays broad absorption bands in the range of 3200-3600 cm^{-1}, corresponding to O-H stretching vibrations indicative of hydroxyl groups found in cellulose and hemicellulose. Around 2900 cm^{-1}, all samples exhibit peaks due to C-H stretching vibrations from aliphatic groups. The fingerprint region (500-1500 cm^{-1}) shows a variety of peaks, particularly strong around 1030-1150 cm^{-1}, due to C-O stretching vibrations typical of cellulose and hemicellulose, and around 1315-1375 cm^{-1}, indicating C-H bending vibrations. Distinct absorption bands near 1740 cm^{-1} are present in Morinda and Ipomoea spectra, attributed to C=O stretching vibrations, suggesting acetyl or ester groups. Additional notable peaks include those around 1500-1600 cm^{-1} for aromatic ring vibrations from lignin and around 1235 cm^{-1} for C-O-C stretching

vibrations linked to ether linkages in lignin. Specifically, Tamarindus indica shows unique patterns in the fingerprint region, Morinda citrifolia exhibits distinct peaks around 1740 cm^{-1} indicating higher acetyl or ester content, Ipomoea staphylina displays prominent O-H and C=O stretching, and Tinospora cordifolia has a smoother spectrum with less pronounced fingerprint region peaks, suggesting different structural compositions. These spectra provide valuable insights into the functional groups and chemical bonds in the fibers, crucial for understanding their mechanical properties and potential applications in composite materials.

Morphology Analysis

The morphological analysis of various composites specimens shown in Figure.7 evaluated in this present study. It's possible to observe impurities on fiber plate surfaces as well as the presence of parenchyma cells. Figure 8(a) shows the adhesion improved morinda-citrifolia fibers. It's clearly shows the impurities bonded in the composite fiber, which shows addition layers on fiber surface, Figure 8(b) shows epoxy with tamarindus–indica composite fractograpy image.

The use of the coupling agent removes the aggregation and shows a remarkable sense of pull out fibers in this composite. Figure 8(c) shows the surface morphology of epoxy tinospora cordifolia composite. The images revealed that the reinforced tinospora fiber had improved adhesion with matrix and associate well in load sharing phenomenon. Figure 8(d) shows ipomoea staphylina fiber with epoxy resin composite. The matrix debris still available on the surface of the fibers after the test was conducted. This shows improved adhesion nature of fiber with epoxy.

The Scanning Electron Microscope (SEM) images illustrate the surface morphology of various epoxy-based natural fiber composites, revealing details about the distribution, bonding, and surface characteristics of the fibers within the epoxy matrix. The Epoxy Morinda Citrifolia Composite (EMC) shows smooth and cylindrical Morinda citrifolia fibers with some particles and debris on the surface, indicating potential weak fiber-matrix bonding areas. The dense network of Tamarindus indica fiber in the Epoxy Tamarindus Indica Composite (ETI) exhibits surface roughness and occasional spaces, indicating possible weak interfacial bonding locations but acceptable mechanical interlocking. Smooth Tinospora cordifolia fiber are evenly dispersed throughout the matrix of the Epoxy Tinospora Cordifolia Composite (ETC), while surface particle matter suggests insufficient wetting or bonding. In locations where interfacial bonding is weak and mechanical integrity may be compromised, the Epoxy Ipomoea Staphylina Composite (EIS) exhibits an uneven fiber network with visible holes and gaps surrounding some Ipomoea staphylina fibers. Overall, the SEM pictures shed important light on the microstructural features of these composites, highlighting the necessity of sufficient fiber-matrix bonding and good fiber dispersion for the best mechanical qualities. The presence of cavities, gaps, and particle matter indicates potential locations where the production process should be improved upon to increase the performance of composites.

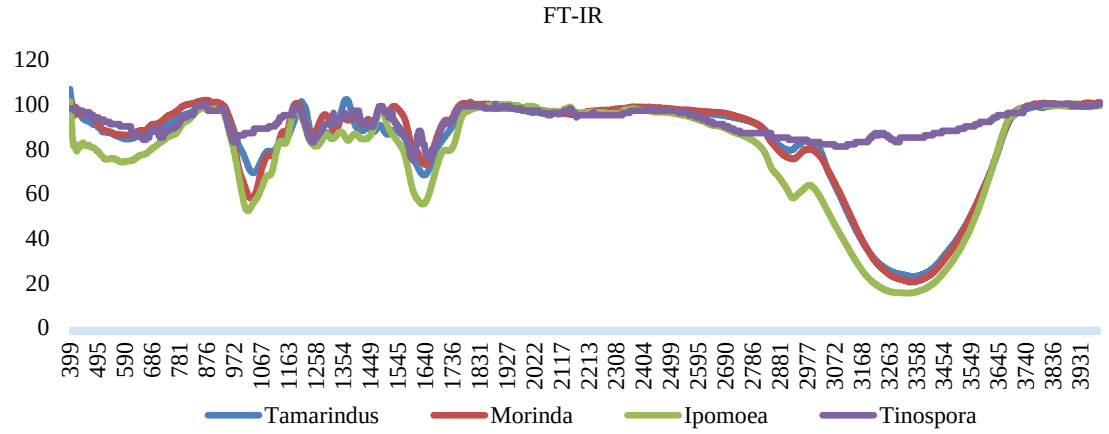

Figure 7. FTIR analyses of Tamarindus, Morinda, Ipomoea, Tinospora bio fibers

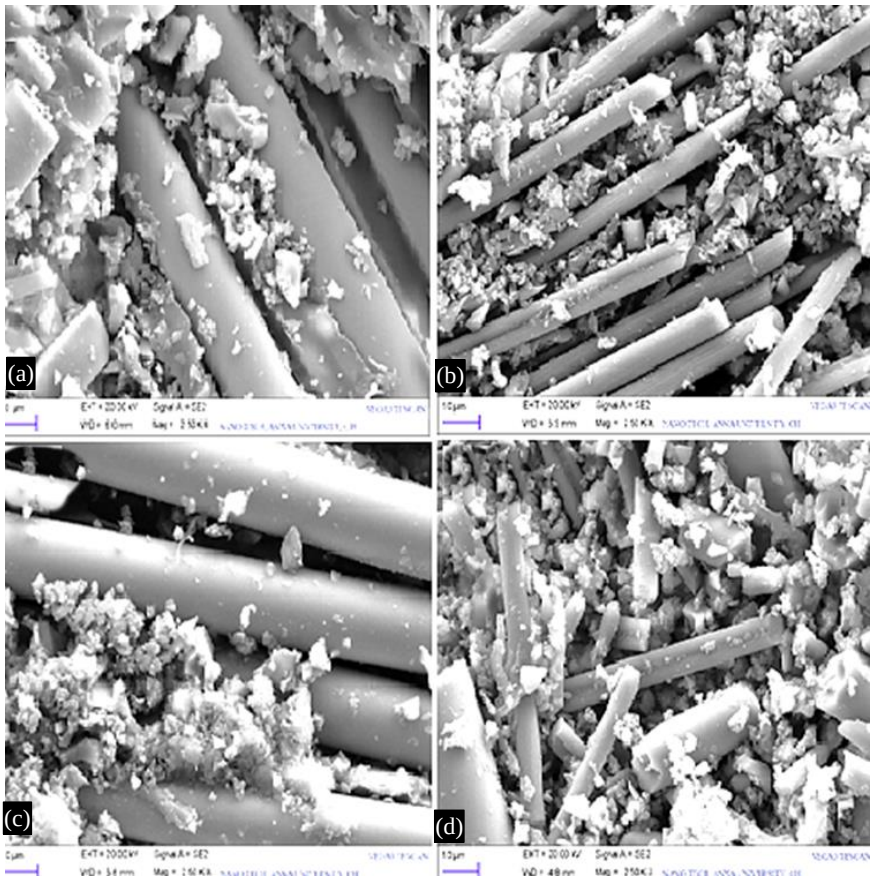

Figure 8. SEM analyis of a) EMC, b) ETI, c) ETC and d) EIS bio fiber composite.

Numerical Investigation of Natural Fiber Composite Panel

For the numerical analysis only ETI and EMC were considered, ETC and EIS were neglected due to its very lower mechanical property values in the experimental work.

The contour plots presented in Figure 9 depicts the distribution of shear elastic strain (XY element) for a composite material subjected to varying compressive loads, specifically 3000 N, 4000 N, and 5000 N. In the overall coordinate system, each graphic displays the distribution of strain in millimetres per millimetre across the upper and bottom surfaces of the material at a given time point (1 second). The shear elastic strain for the 3000 N load (03:13 PM) is between -0.00028071 mm/mm (blue) and 0.00028071 mm/mm (red). The green colour indicates that the core region is essentially intact, while greater stress concentrations are seen at the corners, showing severe deformation in these places. The strain levels vary from -0.00037428 mm/mm to 0.00037428 mm/mm under the 4000 N load (03:11 PM). The core region still shows minor strain, but the additional load causes larger strain values and more noticeable deformation at the corners. The strain distribution for the 5000 N load (03:10 PM) is -0.00046785 mm/mm to 0.00046785 mm/mm. The strain values climb as the load is increased further, suggesting increasing deformation and stress concentrations near the margins of the material. All things considered, these contour plots show a very evident trend: when the compressive load rises, so do the highest and lowest shear elastic strain values, leading to increased deformation, especially at the material's corners. The material's edges are especially susceptible to deformation during compressive pressures, as evidenced by the core region's relative stability under low strain. Comprehending the strain distributions is essential for forecasting the behaviour of materials under stress, pinpointing possible locations of failure, and refining material design to enhance longevity and efficacy in compressive force-affected applications.

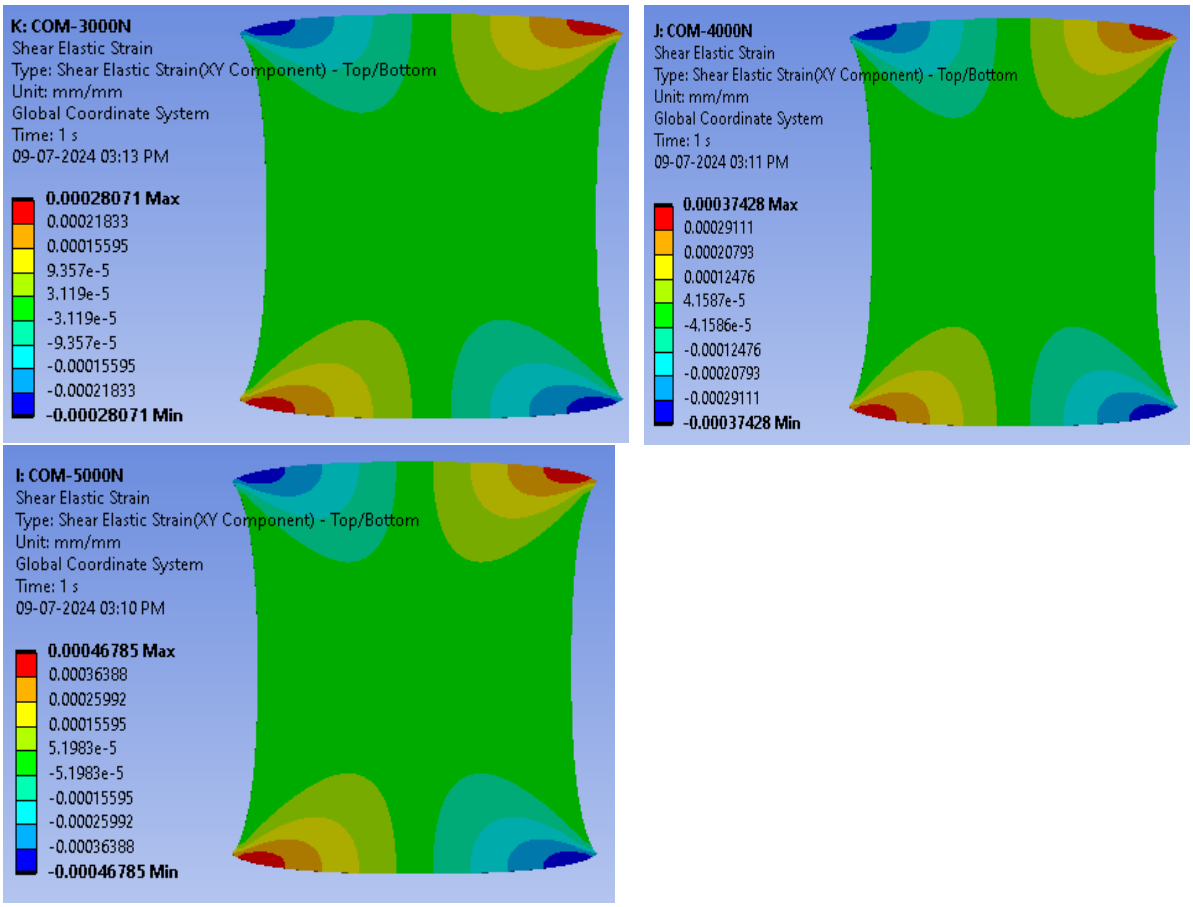

Figure 9. Analysis of shear elastic strain variation under compreesive loads.

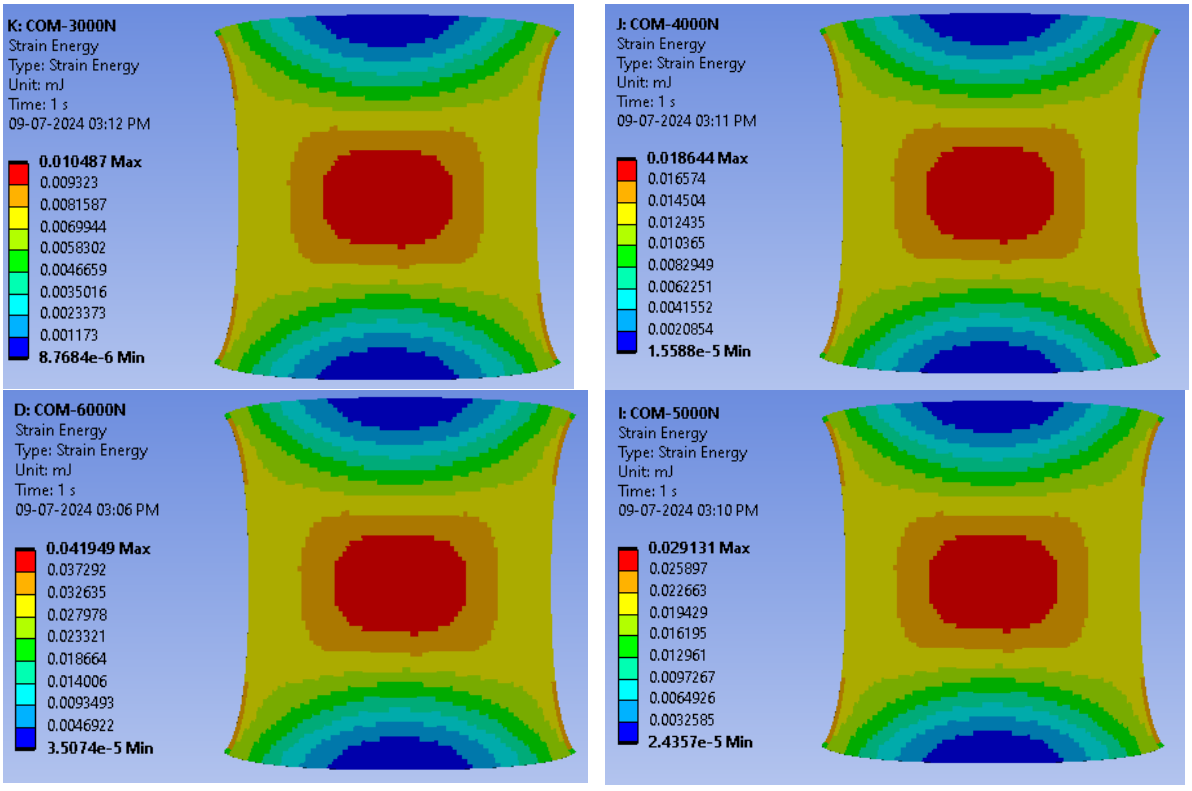

Figure 10. Analysis of strain energy variation under compreesive loads.

The above Figure 10 shows strain energy variation of the composite material with different compressive loads of 3000 N, 4000 N, 5000 N, and 6000N. At 3000 N, the strain energy varies between 8.7684e-6 mJ to 0.010487 mJ. The middle region exhibits the highest energy, signifying substantial deformation. The strain energy range expands from 1.5588e-5 mJ to 0.018644 mJ when the load increases to 4000 N. A larger red area in the centre indicates improved energy storage because of higher deformation. The strain energy range is further increased in the 5000 N load plot, from 2.4357e-5 mJ to 0.029131 mJ, with the outlying regions displaying elevated energy levels and the middle region storing even more energy. In conclusion, the strain energy under a 6000 N load varies from 3.5074e-5 mJ to 0.041949 mJ. The core region shows significant deformation and storage of energy, while the edges and corners also show higher energy levels than under lower pressures. These plots show that the material's strain energy increases with increasing compressive load, especially in the centre region, which is where compressive stress has the greatest impact. Comprehending the strain energy distributions is essential for forecasting the behaviour of materials under stress, pinpointing possible locations of failure, and refining material design to enhance the resilience and efficacy of composite materials in compressive force applications.

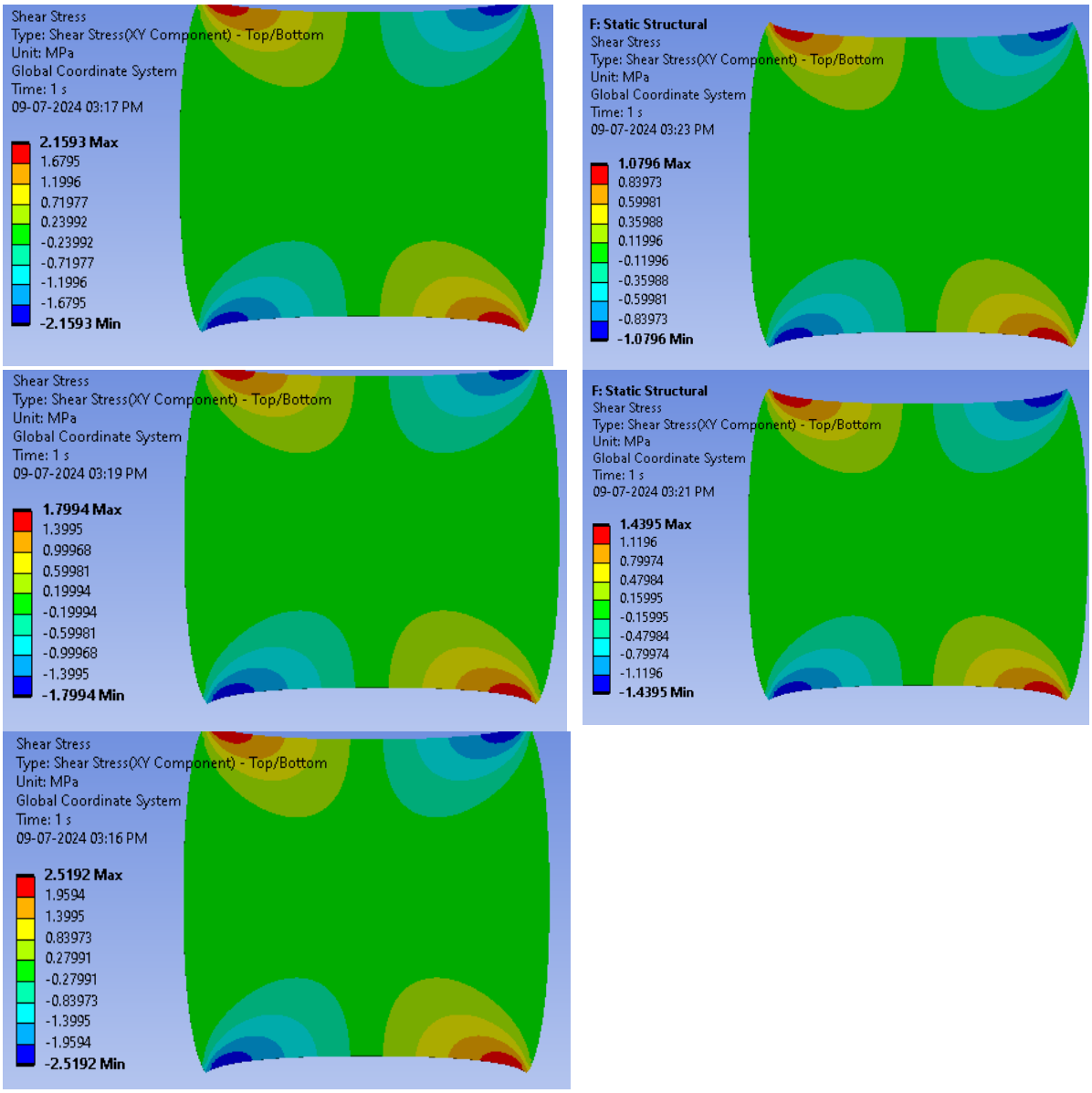

Figure 11. Analysis of shear stress distribution under compreesive loads.

For a composite material, the contour plots supplied show the shear stress distribution under different compressive loads in Figure 11: 3000 N, 4000 N, 5000 N, 6000 N, and 7000 N. In the overall coordinate system, each graphic displays the distribution of shear stresses in MPa across the upper and bottom surfaces of the material at a given time point (1 second). The shear stress for the 3000 N load is -1.0796 MPa (blue) to 0.8399 MPa (red). The core portion, as seen by the green colour, is essentially intact, but higher stress intensities are seen around the corners, suggesting severe deformation in these places. The stress levels vary between -1.4195 MPa to 1.1176 MPa under the 4000 N load. The core region still shows minor stress, but the additional load causes greater stress levels and more noticeable deformation around the corners. The shear stress variation for the 5000 N load is -1.7994 MPa to 1.3994 MPa. The stress values grow in response to the additional load, suggesting increasing deformation and stress concentrations near the margins of the material. The stress varies from -2.1595 MPa to 1.7995 MPa at 6000 N. Shear stress in the core region rises, and the deformation structure becomes more obvious, especially around the edges and corners. Lastly, the shear stress varies between -2.5192 MPa to 2.1592 MPa for the 7000 N load. The material experiences considerable deformation and stress concentrations at the corners and edges under this load, resulting in the greatest stress values. The middle region, on the other hand, continues to endure lower stress levels. All things considered, these contour plots show a very evident trend: when the compressive load rises, so do the maximum and lowest shear stress values, which leads to more substantial deformation, especially at the material's corners. The material's edges are highly susceptible to deformation during compressive pressures, as evidenced by the central region's relative stability under low stress. Comprehending the stress distributions is essential for forecasting the behaviour of materials under stress, pinpointing possible locations of failure, and refining material design to enhance longevity and efficacy in compressive force applications.

The total deformation (mm) of Tamarindus indica and Morinda citrifolia with various compressive loads (N) are shown in Figure 12. The Tamarindus indica, indicating minimum deformation is 0.016 mm up to 6000 N compressive loads. From this Tamarindus indica’s possess maximum resistance to deformation due to inner structural integrity. But Morinda citrifolia shows the highest deformation 0.032 mm at 6000N compressive loads due to its lower resistance against the compressive stresses. From this result it is clear that Tamarindus indica is more rigid and stiffer to maintain its shape under load, but Morinda citrifolia possess more dampening and flexible property due to its deformation.

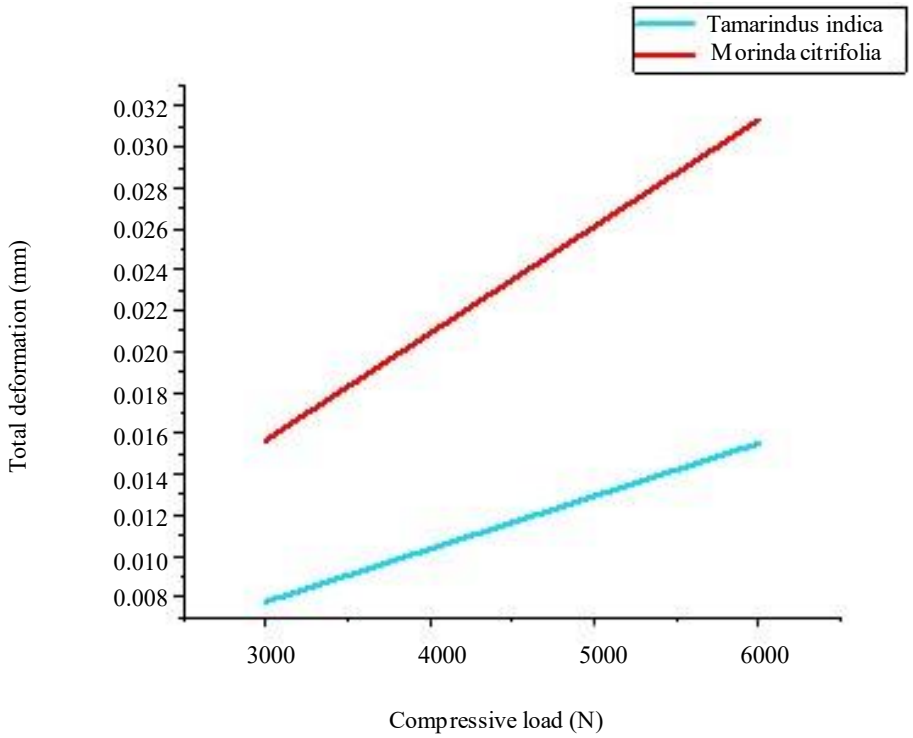

Figure 12. Comparison of total deformation under compreesive loads.

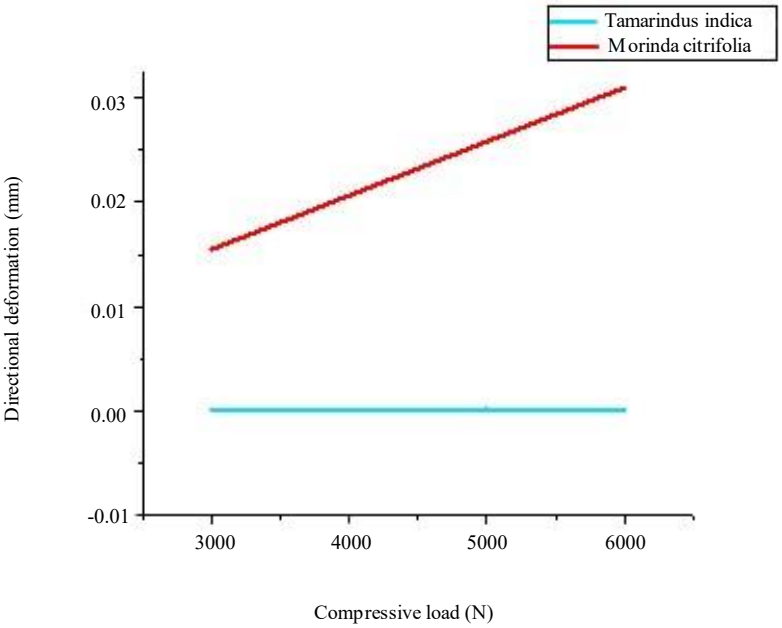

Figure 13. Comparison of directional deformation under compreesive loads.

The relationship between directional deformation (in mm) and compressive load (in N) for two composite materials—Tamarindus indica and Morinda citrifolia—is shown in Figure 13. These two materials behave differently mechanically when subjected to compressive force. The light blue line, Tamarindus indica, shows very little directional deformation as compressive loads increase. It provides the strong resistance to compressive deformation from the load 3000N to 6000N. Due to this behaviour it could gives the better structural integrity and stiffness in the compressive load. So the tamarindus indica is the optimum material for construction application to protect the shape and rigidity under the compressive load. In other case morinda citrifolia exhibits an elevated directional deformation against the compressive force. The deformation varies from 0.01 mm to 0.03 mm according to load variation from 3000N to 6000N, because of its internal molecular bonding and composition. So, the Morinda citrifolia's can be used at isolating application where the flexibility is more dominant.

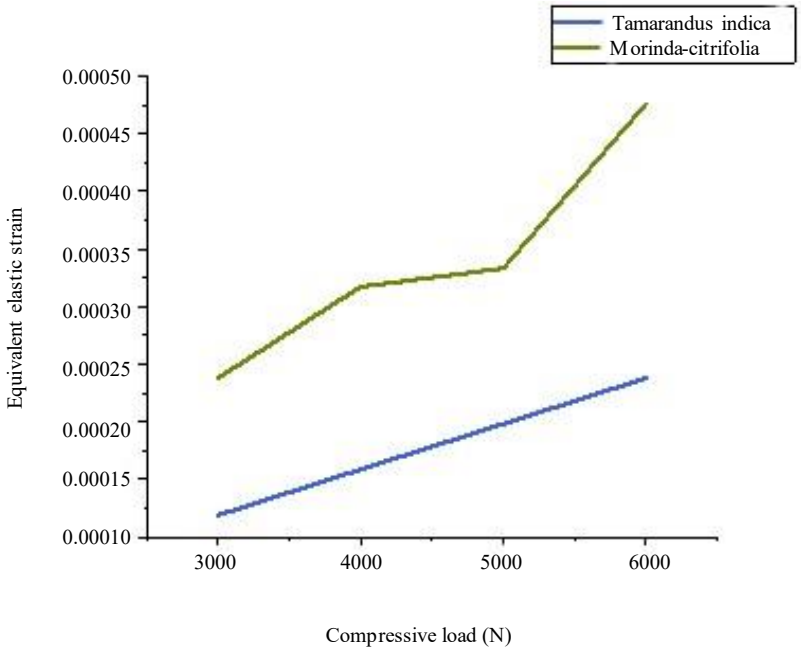

Figure 14. Comparison of equivalent elastic strain under compreesive loads.

The above Figure 14 indicates the equivalent elastic strain variation of Tamarindus indica and Morinda citrifolia with different compressive load from 3000 N to 6000 N. Tamarindus indica indicates a strong consistent elastic behaviour and decreased deformability with a linear rises in strain from 0.00010 at 3000 N to 0.00015 at 6000 N. In the case of Morinda citrifolia possess the higher strain approximately from 0.00025 at 3000 N to 0.00045 at 6000N and it shows morinda possess high deformation and sensitiveness against the load variation. As well as Tamarindus indica possess the less strain and low sensitivity against the load.

The Figure 15 shows the strain energy variation against the compressive load for Tamarindus indica & Morinda citrifolia. The strain energy for Tamarindus indica rises uniformly from about 0.005 mJ at 3000 N to about 0.015 mJ at 6000 N, representing a steady and medium capacity for energy absorption. In another case, the strain energy of morinda citrifolia, rises faster rate from 0.015 mJ at 3000 N to 0.040 mJ at 6000 N. This gives that comparison to Tamarindus indica, Morinda citrifolia has a greater capability for energy absorption against the compressive stresses. Morinda citrifolia seems to be better in energy absorption, so that it can be used in damping application to absorb the vibration energy.

Figure 16 graph plotted against the location along the x-axis, the graph displays the total deformation, measured in millimetres (mm), of Tamarindus indica during various tensile strains. Along the position, the deformation increases linearly with the tensile load. The distortion begins at 0 mm and increases progressively to around 0.01 mm in the longest place during a 3000 N load. Similar trends are shown with the 4000 N load, although there is more deformation—up to 0.015 mm. Even greater deformation is brought up by the 5000 N load, which peaks at about 0.02 mm. The maximum deformation, which culminates at approximately 0.03 mm, is caused by the 6000 N load. The material consistently stretches over its length when applied tensile loads are applied, as indicated by the linear relationship between position and deformation. This illustrates the elastic behaviour of the material and its ability to deform under a range of tensile stresses: the larger the applied load, higher the total deformation. Tamarindus indica's mechanical qualities and applicability for applications needing particular deformation characteristics during tensile loading require a grasp of this information.

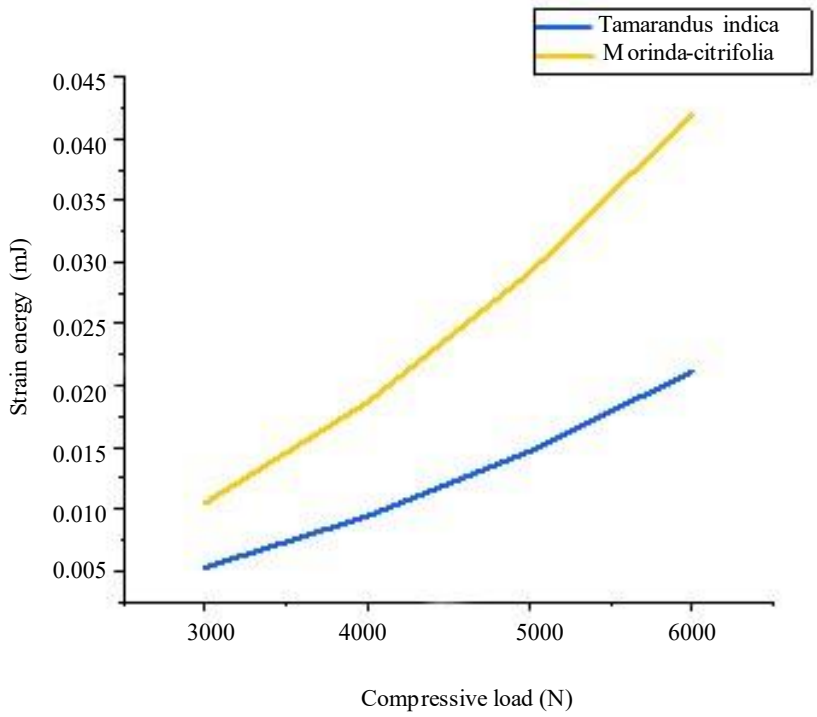

Figure 15. Comparison of Strain energy under compreesive loads.

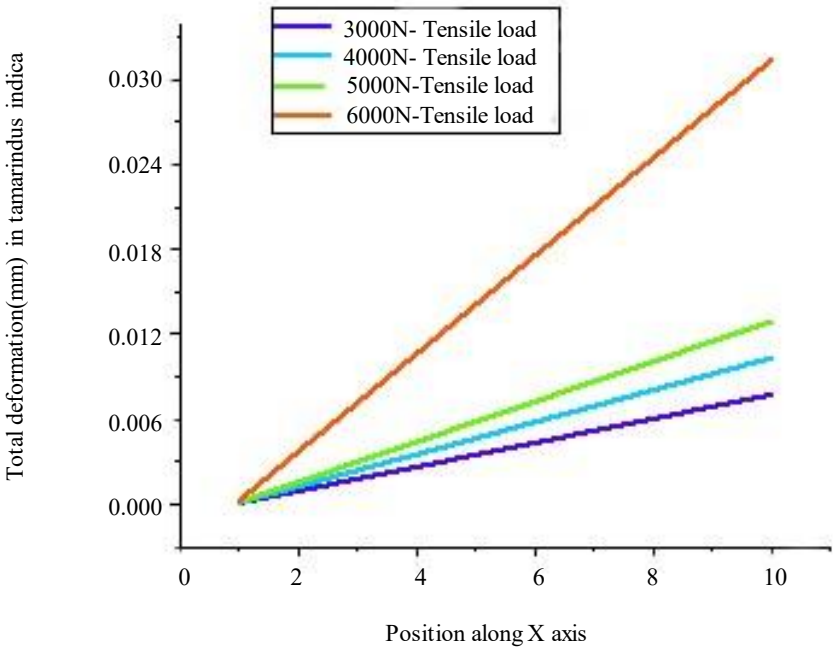

Figure 16. Variation of total deformation with different tensile loading.

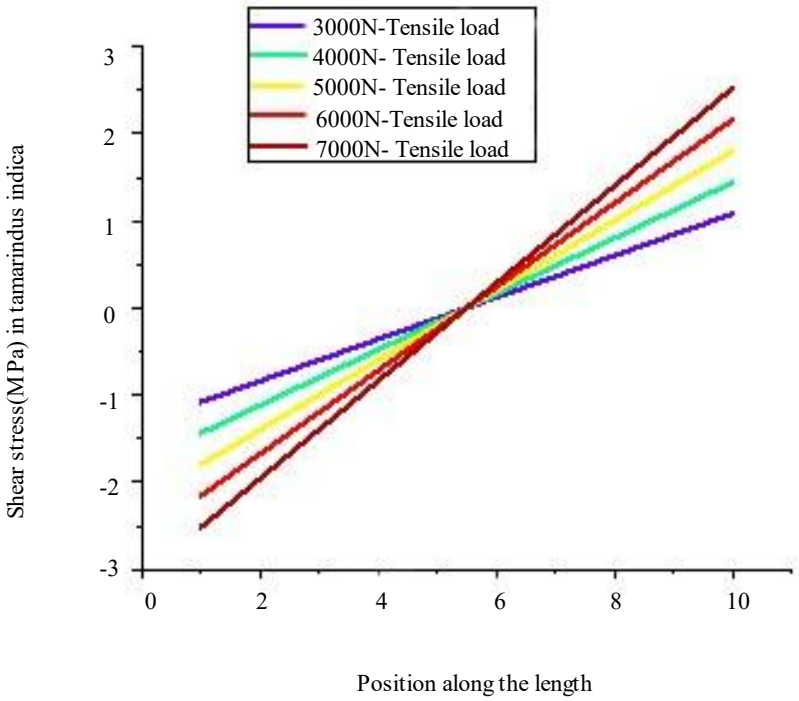

Figure 17. Variation of shear stress in ETI composite with different tensile loading.

The distribution of shear stress under various tensile loads from 3000 N to 7000 N is shown in Figure 17 throughout the entire length of Tamarindus indica fiber. Tensile loads are represented by the following coloured lines: 7000 N (brown), 5000 N (yellow), 6000 N (red), 4000 N (cyan), and 3000 N (purple). Every line, which crosses the y-axis at zero and extends symmetrically in both positive and negative directions, depicts the linear connection among the position throughout the length and the shear stress. The slope of the lines sudden rise with respect to tensile load indicates higher value of shear stress. At tensile load application, the material may attain homogeneous shear stress along the length, according to this uniform and symmetric distribution.

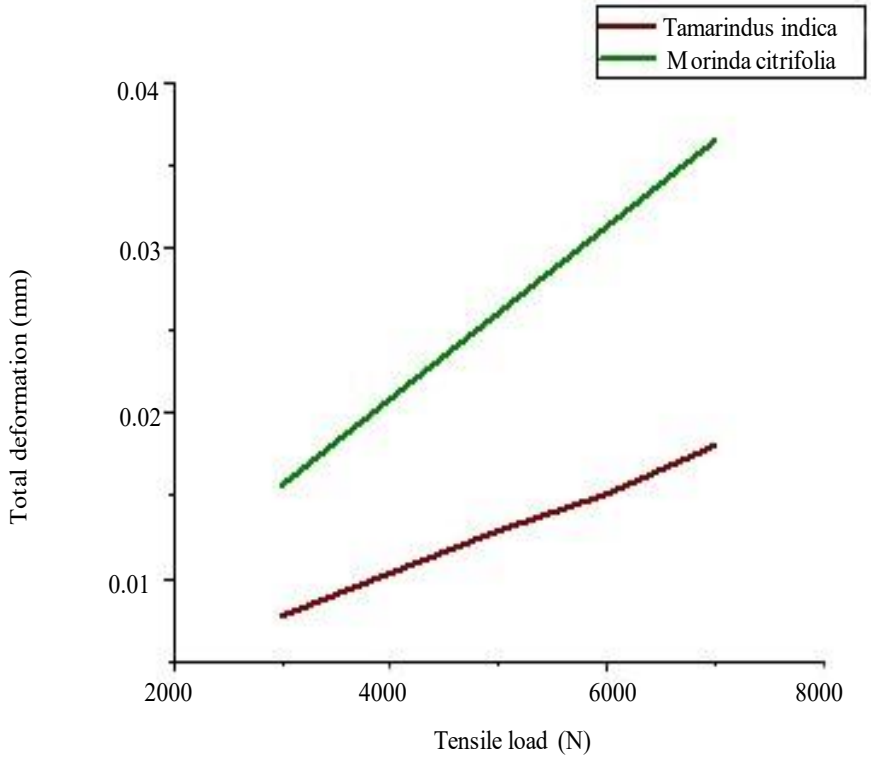

Figure 18. Compression of total deformation in EMC and ETI composite under tensile loading.

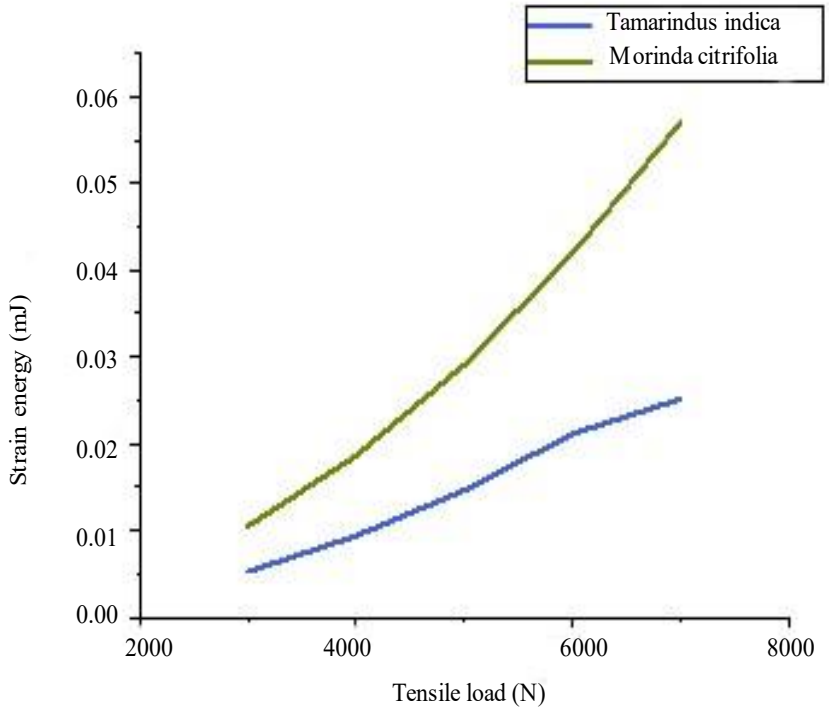

Figure 19. Compression of strain energy in EMC and ETI composite under tensile loading.

The total deformation with different tensile loads ranging from 2000N to 7000N as shown in Fig. 19. While the total deformation of two materials rises with increase in the tensile load, Morinda citrifolia shows higher deformation at all stress value than Tamarindus indica. For example, at 7000 N, Tamarindus indica barely deforms about 0.015 mm, but Morinda citrifolia attains a deformation of about 0.035 mm. This suggests that Morinda citrifolia is less stiff or more elastic than Tamarindus indica, as it is more prone to deformation during tensile stress. Although the deformation rise for both materials is linear, indicating consistent elastic behaviour, the differing slopes emphasise the unique mechanical features of each material. Tamarindus indica would be preferred in scenarios requiring reduced deformation, while Morinda citrifolia could be appropriate for applications where increased flexibility and deformation are favourable. This contrast is important for applications requiring certain deformation properties.

Tamarindus indica and Morinda citrifolia are the two materials whose strain energies (measured in millijoules, mJ) are shown in Figure 19 under a range of tensile loads, from 2000 N to 7000 N. When tensile loads increase, both materials show a rise in strain energy; however, Morinda citrifolia exhibits significantly greater strain energy at every load level than Tamarindus indica. For instance, Tamarindus indica reaches roughly 0.02 mJ of strain energy at 7000 N, while Morinda citrifolia reaches about 0.06 mJ. This suggests that Morinda citrifolia is more flexible or less stiff than Tamarindus indica because it absorbed more energy under tensile stress. Tamarindus indica is good for applications require a lower absorption of energy, while Morinda citrifolia is good for requiring high energy absorption and flexibility applications.

CONCLUSION

From the overall investigation of the mechanical behaviour of following materials, such as EMC, ETI, ETC and EIS along with comparison of Tamarindus indica and Morinda citrifolia delivers information about their suitable applications. From the analysis it is clearly shows that ETI possess good mechanical properties such as higher tensile strength (8 MPa), flexural load capability (0.35 kN), and compressive load capability (6 kN). Due to these properties ETI is suitable material for more weight-bearing and high strength applications. In another case ETC possess lesser value of flexural load carrying capacity (0.1 kN) and tensile strength (2 MPa). Instead of having the highest Shore D hardness value(60), it sustain poorly for all load condition shows that not suitable for high-stress applications. The comparison of Tamarindus indica, Morinda citrifolia shows that remarkably higher total deformation and equivalent elastic strain at various compression and tension loads. It is clear that Morinda citrifolia possess high flexibility and low stiffness than Tamarindus indica. In the Strain energy analysis indicates the Morinda citrifolia capable of high energy absorption by an influence of tensile stress, So that it can be used as a dampening or cushioning materials to absorb the vibrational energy.

Funding Details

This research did not receive any specific grant from funding agencies in the public, commercial, or not-for-profit sectors.

REFERENCES

1. Smith A, Johnson B, Brown C. Mechanical properties of natural fiber composite materials: a review. J Compos Mater. 2024;60:1-10.
2. Walker P, Hall Q, Young R. Mechanical properties of natural fiber composite materials: a review. J Compos Mater. 2024;60:1-10.
3. Phillips E, Evans F, Turner G. Mechanical properties of natural fiber composite materials: a review. J Compos Mater. 2024;60:1-10.
4. Richardson T, Rogers U, Butler V. Mechanical properties of natural fiber composite materials: a review. J Compos Mater. 2024;60:1-10.

5. Coleman I, Patterson J, Bell K. Mechanical properties of natural fiber composite materials: a review. J Compos Mater. 2024;60:1-10.
6. Crawford X, Gray Y, Cole Z. Mechanical properties of natural fiber composite materials: a review. J Compos Mater. 2024;60:1-10.
7. Johnson B, Moore C, Harris D. Mechanical properties of natural fiber composite materials: a review. J Compos Mater. 2024;60:1-10.
8. Hall Q, Wilson R, Campbell S. Mechanical properties of natural fiber composite materials: a review. J Compos Mater. 2024;60:1-10.
9. Miller D, Davis E, Wilson F. Analysis of mechanical properties in hemp fiber composites. Compos Struct. 2023;59:11-20.
10. Allen S, King T, Wright U. Analysis of mechanical properties in hemp fiber composites. Compos Struct. 2023;59:11-20.
11. Parker H, Campbell I, Nelson J. Analysis of mechanical properties in hemp fiber composites. Compos Struct. 2023;59:11-20.
12. Simmons W, Peterson X, Brooks Y. Analysis of mechanical properties in hemp fiber composites. Compos Struct. 2023;59:11-20.
13. Russell A, Morrison B, Elliott C. Analysis of mechanical properties in hemp fiber composites. Compos Struct. 2023;59:11-20.
14. Walker E, Clark F, Evans G. Analysis of mechanical properties in hemp fiber composites. Compos Struct. 2023;59:11-20.
15. Moore G, Taylor H, Anderson I. Mechanical behavior of jute fiber reinforced composites. Compos Part B Eng. 2022;58:21-30.
16. Scott V, Green W, Baker X. Mechanical behavior of jute fiber reinforced composites. Compos Part B Eng. 2022;58:21-30.
17. Foster Z, Ward A, Bailey B. Mechanical behavior of jute fiber reinforced composites. Compos Part B Eng. 2022;58:21-30.
18. Rogers D, Hamilton E, Graham F. Mechanical behavior of jute fiber reinforced composites. Compos Part B Eng. 2022;58:21-30.

